

## Electronic Supplementary Information

### **New cell membrane-anchored near-infrared fluorescent probes for viscosity monitoring**

Ya Liu,<sup>ab</sup> Xiaohua Li,<sup>\*ab</sup> Wen Shi<sup>ab</sup> and Huimin Ma<sup>\*ab</sup>

*<sup>a</sup> Beijing National Laboratory for Molecular Sciences, Key Laboratory of Analytical Chemistry for Living Biosystems, Institute of Chemistry, Chinese Academy of Sciences, Beijing 100190, China*

*<sup>b</sup> University of Chinese Academy of Sciences, Beijing 100049, China*

*E-mail: lixh@iccas.ac.cn, mahm@iccas.ac.cn*

### **Contents**

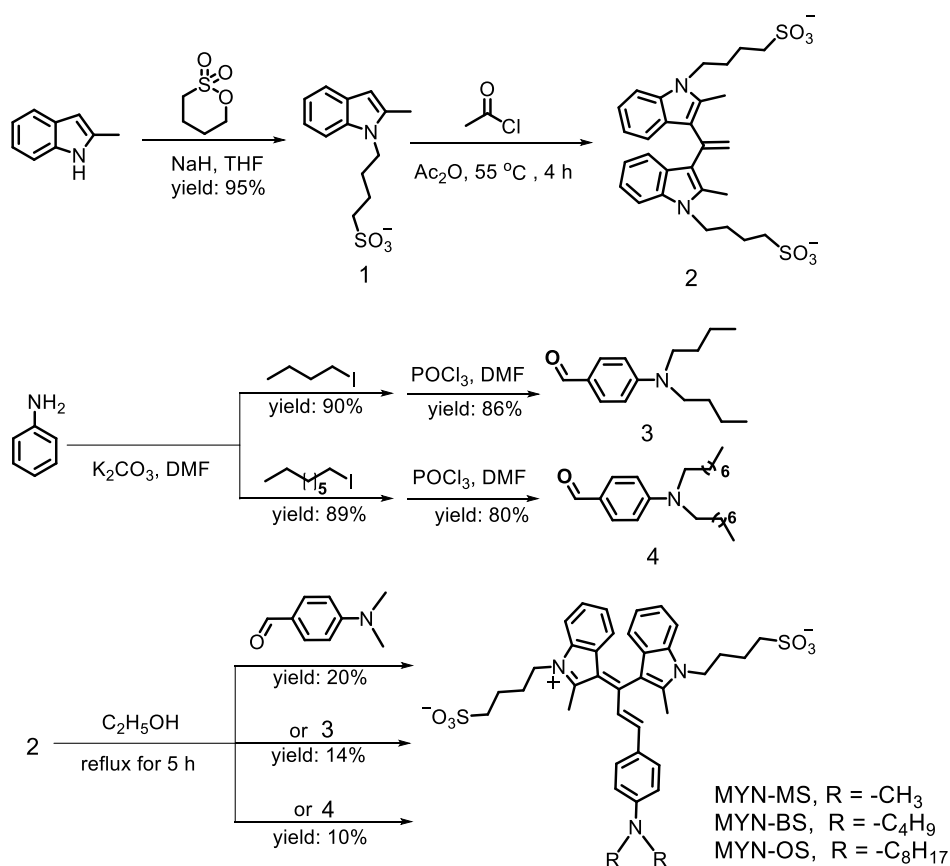
- 1. Apparatus and reagents**
- 2. Syntheses and characterizations**
- 3. General procedure for viscosity detection**
- 4. Cell culture and cytotoxicity assay**
- 5. Cell fluorescence imaging**
- 6. Colocalization experiments**
- 7. Additional tables and figures**
- 8. References**

## 1. Apparatus and reagents

<sup>1</sup>H NMR and <sup>13</sup>C NMR spectra were obtained on Bruker Fourier 700 spectrometer. Electrospray ionization mass spectra (ESI-MS) were measured with a LC-MS 2010A instrument (Shimadzu, Japan). High-resolution electrospray ionization mass spectra (HR-ESI-MS) were acquired on an APEX IV FTMS instrument (Bruker, Daltonics). UV-vis absorption spectra and fluorescence data were collected on TU-1900 (Beijing, China) spectrometer and Hitachi F-4600 spectrophotometer in 1-cm quartz cell. For cytotoxicity experiments, the SpectraMax i3 microplate reader (Molecular Devices, USA) was employed. Fluorescence imaging of cells was run on an FV 1200-IX83 confocal laser scanning microscope (Olympus, Japan) equipped with Olympus software (FV10-ASW).

1-Iodobutane, 1-iodooctane, 2-methylindole, 1,4-butane sultone, sodium hydride, 4-(dimethyl amino) benzaldehyde and glycerol were obtained from InnoChem Science & Technology Co. Ltd. Acetyl chloride and 3-(4,5-dimethyl-2-thiazolyl)-2,5-diphenyl-2H-tetrazolium bromide (MTT) were purchased from Sigma-Aldrich, and phosphate buffered saline (PBS: 137 mM NaCl, 2.7 mM KCl, 8.1 mM Na<sub>2</sub>HPO<sub>4</sub>, 1.5 mM KH<sub>2</sub>PO<sub>4</sub>; pH 7.4) from Biological Industries. Nile red and 3,3'-dioctadecyloxacarbocyanine perchlorate (DIO) were obtained from Thermo Fisher. All cell lines used, Dulbecco's modified Eagle's medium (DMEM) and Roswell Park Memorial Institute (RPMI) 1640 were purchased from KeyGEN BioTECH Co. Ltd., Nanjing, China. DMEM/F12 was purchased from Procell Life Science & Technology Co. Ltd. Newborn calf serum (NBS) was obtained from Hangzhou Sijiqing Biological Engineering Materials Co. Ltd. Fetal bovine serum (FBS) was obtained from Invitrogen Corporation, and oxidized low-density lipoprotein (ox-LDL) from Jingke Chemistry. TMN355 and ezetimibe were purchased from MedChem Express. Ultrapure water (over 18 MΩ·cm) was made by a Milli-Q reference system (Millipore). The storage solutions of probes (1 mM) were prepared in water and kept in small aliquots at -80 °C.

## 2. Syntheses and characterizations



**Scheme S1.** Syntheses of MYN-MS, MYN-BS and MYN-OS.

**Syntheses of compounds 1 and 2.** These two compounds were prepared following the previously reported method.<sup>1</sup> In brief, 1, 4-butane sulfonate (2 mmol, 272 mg) was added to a solution of 2-methylindole (2 mmol, 532 mg) and NaH (2.1 mmol, 84 mg) in 10 mL dry tetrahydrofuran at 0 °C, and then the mixture was stirred at 100 °C for 2 h. After cooling, an appropriate amount of isopropanol was introduced into the solution until the white solid was completely precipitated. The white solid was collected by filtration and dried to afford a yellowish compound **1**, which was used directly in the next step. Then, 78 mg acetyl chloride (1 mmol) was added dropwise to 10 ml of acetic anhydride containing compound **1** (532 mg, 2 mmol). The mixture was stirred at 55 °C for 4 h under the protection of nitrogen. The resulting solution was evaporated under reduced pressure, affording compound **2** as a purple-red solid, which was directly used for synthesis without further purification.

**Syntheses of compounds 3 and 4.** Compounds **3** and **4** were synthesized according to the previous literature.<sup>2</sup>

**Syntheses of probes MYN-MS, MYN-BS and MYN-OS.** Compound **2** (1 mmol, 557 mg) and 4-(dimethylamino)benzaldehyde (1 mmol, 150 mg), compound **3** (1 mmol, 233 mg), or compound **4** (1 mmol, 345 mg) were dissolved in 20 mL ethanol and refluxed at 90 °C for 4 h under N<sub>2</sub> atmosphere. Then, the solvent was removed by evaporation under reduced pressure, and the crude product was purified using silica gel chromatography with CH<sub>2</sub>Cl<sub>2</sub>/CH<sub>3</sub>OH (v/v, 5:1) as an eluent, affording probe MYN-MS (dark-blue solid, yield: 20%), MYN-BS (dark-blue solid, yield: 14%), or MYN-OS (dark-blue solid, yield: 10%), respectively.

MYN-MS: <sup>1</sup>H NMR (700 MHz, CD<sub>3</sub>OD; Fig. S1): δ 7.87-7.78 (m, 4H), 7.64-7.57 (m, 4H), 7.40-7.28 (m, 2H), 7.25-7.08 (m, 2H), 6.91-6.90 (m, 2H), 4.42-4.33 (m, 4H), 3.31-3.30 (t, 4H, J=7 Hz), 2.87 (m, 4H), 2.39-2.37 (s, 3H), 2.07 (s, 3H), 1.92 (m, 10H). <sup>13</sup>C NMR (175 MHz, CD<sub>3</sub>OD; Fig. S2): δ 162.97, 157.76, 155.52, 150.84, 146.13, 137.78, 135.05, 129.57, 128.45, 126.72, 124.58, 123.46, 122.74, 121.08, 120.52, 119.93, 118.71, 116.06, 112.89, 111.48, 110.79, 50.51, 43.67, 39.16, 28.14, 22.14, 16.96, 15.99, 15.88, 15.77, 13.02, 11.63. HR-ESI-MS: m/z calcd. for MYN-MS (C<sub>37</sub>H<sub>42</sub>N<sub>3</sub>O<sub>6</sub>S<sub>2</sub><sup>-</sup>, [M]<sup>-</sup>), 688.2521; found, 688.2519.

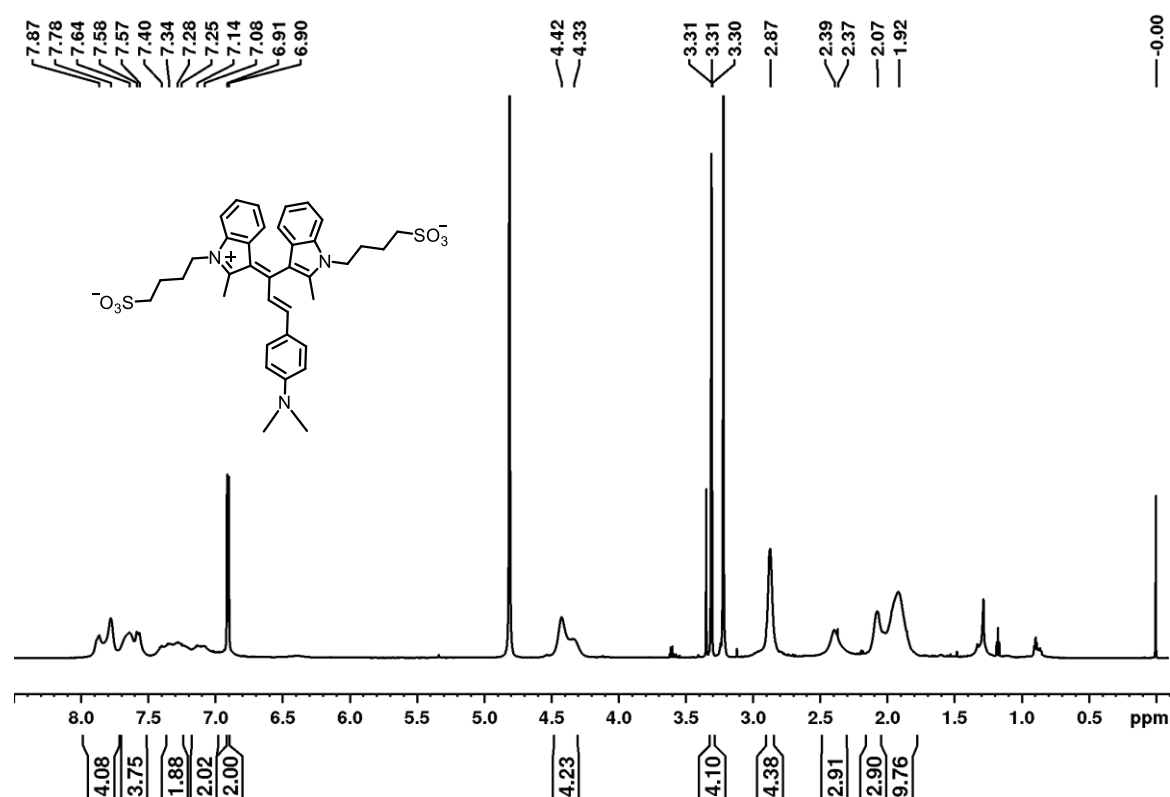


**Fig. S1** <sup>1</sup>H NMR spectrum of MYN-MS (700 MHz, 298 K, CD<sub>3</sub>OD).

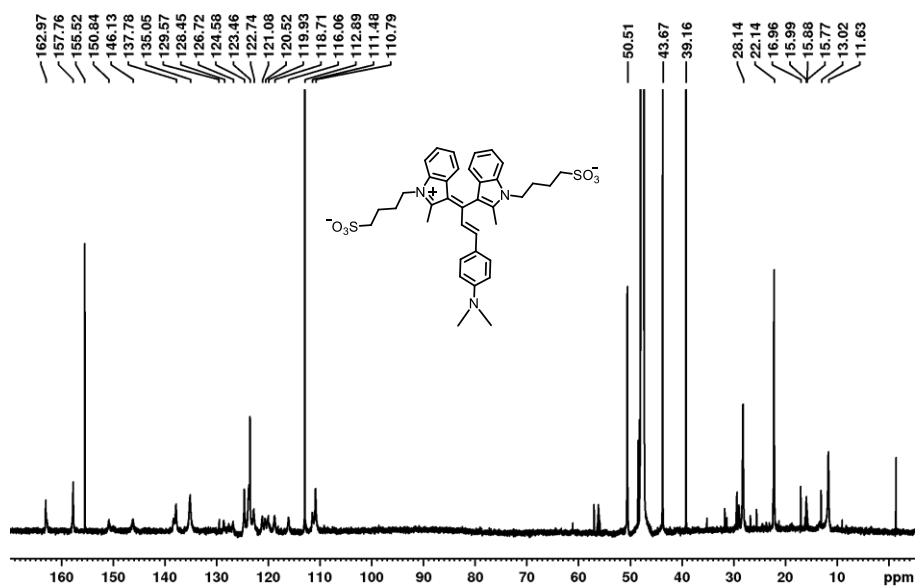


**Fig. S2**  $^{13}\text{C}$  NMR spectrum of MYN-MS (175 MHz, 298 K,  $\text{CD}_3\text{OD}$ ).

MYN-BS:  $^1\text{H}$  NMR (700 MHz,  $\text{CD}_3\text{OD}$ ; Fig. S3):  $\delta$  7.89-7.87 (m, 2H), 7.78-7.62 (m, 2H), 7.60-7.58 (m, 3H), 7.41-7.27 (m, 2H), 7.26-7.09 (m, 3H), 6.90-6.88 (d, 2H,  $J=14$  Hz), 4.42-4.31 (m, 4H), 3.56-3.54 (t, 4H,  $J=14$  Hz), 2.88-2.86 (m, 4H), 2.39 (s, 3H), 2.08 (s, 3H), 1.98-1.86 (m, 8H), 1.69-1.65 (m, 4H), 1.45-1.40 (m, 4H), 1.00-0.98 (t, 6H,  $J=14$  Hz).  $^{13}\text{C}$  NMR (175 MHz,  $\text{CD}_3\text{OD}$ ; Fig. S4):  $\delta$  162.47, 157.57, 154.20, 150.26, 145.65, 138.23, 137.66, 128.55, 126.73, 124.49, 124.36, 123.68, 123.51, 123.17, 122.56, 121.03, 120.32, 118.71, 115.80, 113.12, 111.33, 110.70, 50.89, 50.56, 43.59, 29.43, 29.27, 28.25, 28.06, 22.81, 22.15, 19.74, 12.84, 11.63, 11.43. HR-ESI-MS:  $m/z$  calcd. for MYN-BS ( $\text{C}_{43}\text{H}_{54}\text{N}_3\text{O}_6\text{S}_2^-$ ,  $[\text{M}]^-$ ), 772.3460; found, 772.3453.

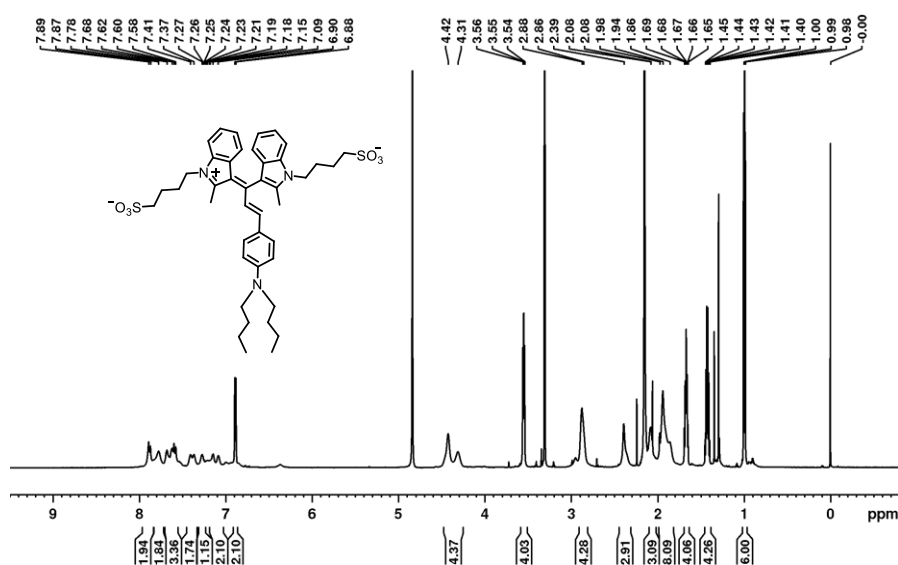


**Fig. S3**  $^1\text{H}$  NMR spectrum of MYN-BS (700 MHz, 298 K,  $\text{CD}_3\text{OD}$ ).

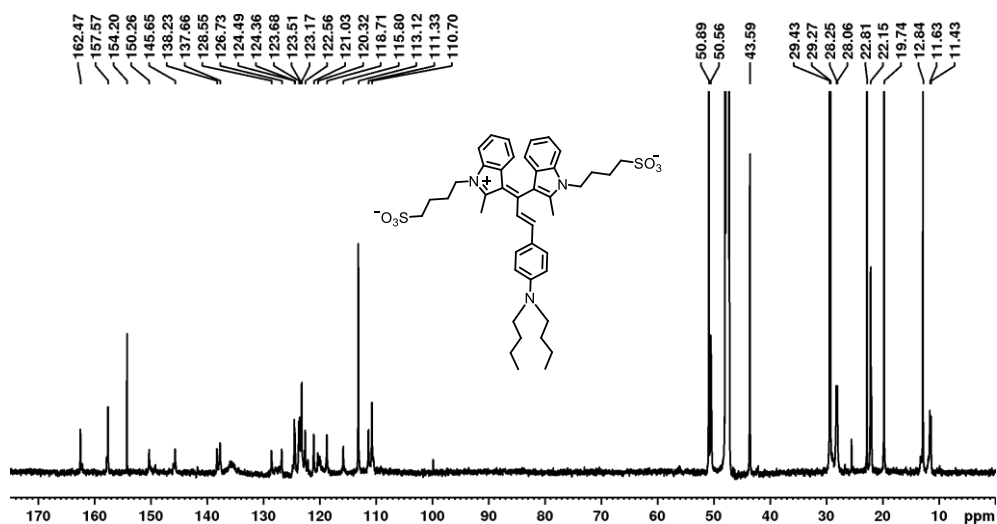


**Fig. S4**  $^{13}\text{C}$  NMR spectrum of MYN-BS (175 MHz, 298 K,  $\text{CD}_3\text{OD}$ ).

MYN-OS:  $^1\text{H}$  NMR (700 MHz,  $\text{CD}_3\text{OD}$ ; Fig. S5):  $\delta$  7.87-7.85 (m, 2H), 7.76-7.67 (m, 2H), 7.62-7.56 (m, 3H), 7.40-7.35 (m, 2H), 7.27-7.25 (m, 1H), 7.23-7.07 (m, 2H), 6.89-6.87 (d, 2H,  $J=14$  Hz), 4.42-4.30 (m, 4H), 3.55-3.52 (t, 4H,  $J=21$  Hz), 2.87 (m, 4H), 2.39 (s, 3H), 2.08 (s, 3H), 1.93 (m, 8H), 1.70-1.66 (m, 4H), 1.38-1.33 (m, 8H), 1.33-1.30 (m, 12H), 0.91-0.89 (s, 6H).  $^{13}\text{C}$  NMR (175 MHz,  $\text{CD}_3\text{OD}$ ; Fig. S6):  $\delta$  162.45, 157.51, 154.20, 150.28, 145.66, 138.23, 137.68, 128.57, 126.73, 124.50, 124.38, 123.68, 123.54, 123.21, 122.57, 121.06, 120.34, 118.72, 115.82, 111.34, 110.71, 56.70, 51.14, 50.54, 43.61, 31.54, 29.12, 28.98, 28.26, 28.08, 27.33, 26.55, 22.29, 22.16, 15.99, 15.88, 13.02, 11.63, 11.45. HR-ESI-MS:  $m/z$  calcd. for MYN-OS ( $\text{C}_{51}\text{H}_{70}\text{N}_3\text{O}_6\text{S}_2^-$ ,  $[\text{M}]^-$ ), 884.4712; found, 884.4703.

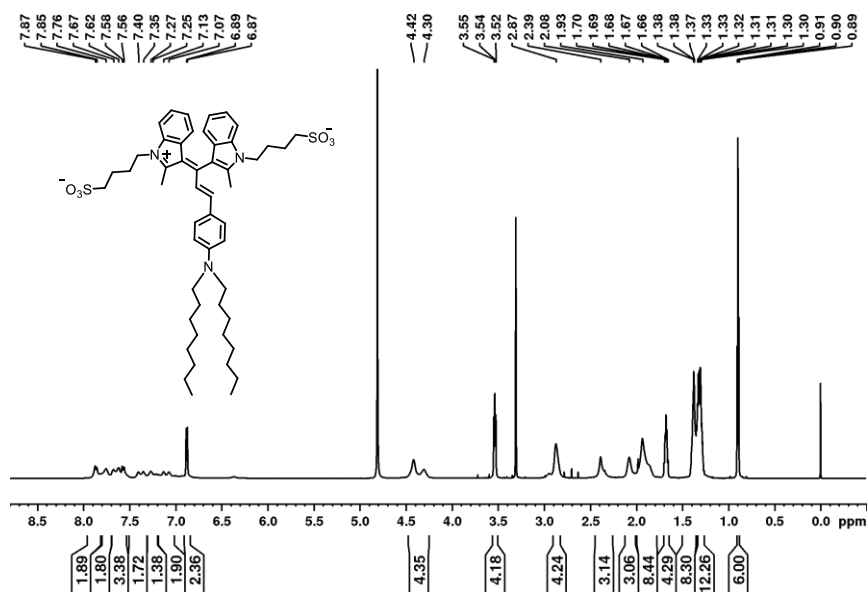


**Fig. S5**  $^1\text{H}$  NMR spectrum of MYN-OS (700 MHz, 298 K,  $\text{CD}_3\text{OD}$ ).

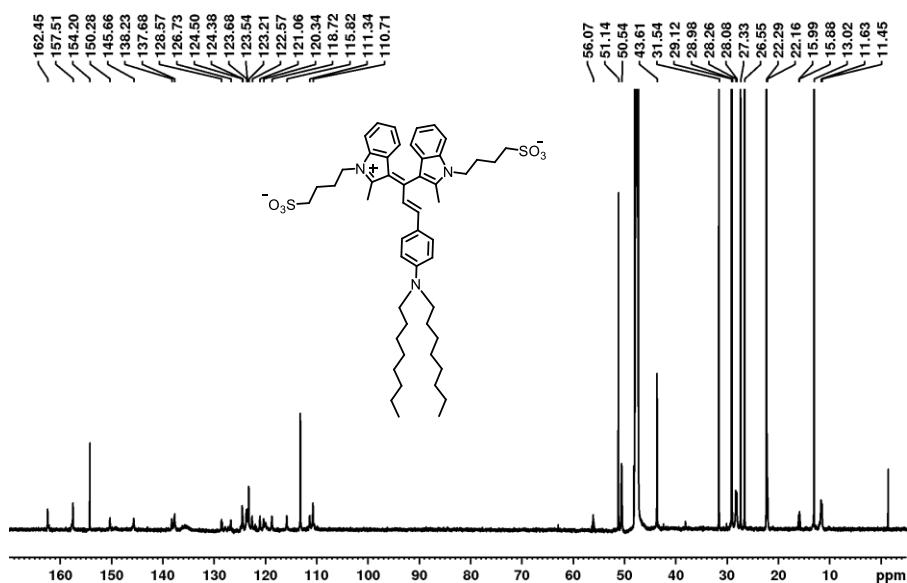


**Fig. S6** <sup>13</sup>C NMR spectrum of MYN-OS (175 MHz, 298 K, CD<sub>3</sub>OD).

### 3. General procedure for viscosity detection

Unless otherwise specified, the final concentration of MYN-MS, MYN-BS and MYN-OS was 5 μM in all *in vitro* experiments. The solutions of these probes with specific concentrations were obtained by adding their stock solutions (1 mM) to the mixture (5 mL) of methanol-glycerol at different volume proportions, or to the sucrose solutions (5 mL) with different concentrations. The resulting solutions were shaken on a constant temperature shaker at 37 °C for 3 h and then cooled to room temperature for eliminating air bubbles. Afterwards, these well-mixed solutions were transferred to a 1-cm quartz cell to measure absorbance against the corresponding reagent blank or fluorescence spectra with  $\lambda_{\text{ex}} = 670$  nm at room temperature (25 °C).

### 4. Cell culture and cytotoxicity assay

AML12 cells were cultured in the medium DMEM/F12 containing 10% FBS, 10 μg/mL insulin and 40 ng/mL dexamethasone. HeLa and HepG2 cells were grown on glass-bottom culture dishes in DMEM supplemented with 10% (v/v) FBS and 1% (v/v) penicillin-streptomycin. RAW264.7 and HT-1080 cells were cultured using RPMI 1640 supplemented with 10% heat-inactivated NBS. All cells were incubated at 37 °C in a humidified 5% CO<sub>2</sub> incubator for 24 h before use in the cell imaging experiments. The cytotoxicity of MYN-BS to the above-mentioned cells was examined by standard MTT assay according to the previous report.<sup>3</sup>

## 5. Cell fluorescence imaging

Prior to adding our probe to cells, the culture medium should be removed. Then, the adherent cells were washed with PBS for three times. For fluorescence imaging, cells in phenol red-free basal medium can be imaged directly after our probe (10  $\mu$ M) was added without washing. The imaging was conducted on the FV 1200-IX83 confocal laser scanning microscope with 635 nm excitation and 650-750 nm emission.

To study the effects of temperature on cell membrane viscosity, the probe and the cells were co-incubated for 20 min at different temperature. Then, the as-treated cells were subjected to confocal imaging. To explore the reversibility of MYN-BS in response to the changes of cell membrane viscosity, the probe and the cells were co-incubated at 37 °C for 15 min, followed by the first imaging; after that, the cells were incubated at 41 °C for another 15 min, and then the second imaging of the cells was performed. These operations were repeated for three times.

To obtain the macrophage-derived foam cells, RAW264.7 cells were co-incubated with ox-LDL at different concentrations (20, 50 and 100  $\mu$ g/mL) for 24 h at 37 °C. Then the cells were imaged according to the above described procedure. For inhibition experiments, the inhibitor (2  $\mu$ M TMN355 or 10  $\mu$ g/mL ezetimibe) and ox-LDL (50 or 100  $\mu$ g/mL) were co-incubated with cells for 24 h before used for imaging. To verify the formation of foam cells, Nile red (1  $\mu$ M) was incubated with the cells for 15 min at 37 °C, followed by imaging.<sup>4</sup> The pixel intensity of the fluorescence images of the cells was calculated and averaged based on at least five cells in each image.

## 6. Colocalization experiments

AML12, HeLa or RAW264.7 cells grown at the bottom of confocal dishes were pre-incubated with 10  $\mu$ M DIO for 20 min at 37 °C in DMEM, followed by washing for three times with PBS. Then, the cells were imaged upon addition of 10  $\mu$ M MYN-BS. In the imaging experiments, the excitation wavelength was 488 nm (for DIO), or 635 nm (for MYN-MS, MYN-BS and MYN-OS); the corresponding fluorescence emissions were collected at 500-550 nm (for DIO) or 650-750 nm (for our probes).

## 7. Additional tables and figures

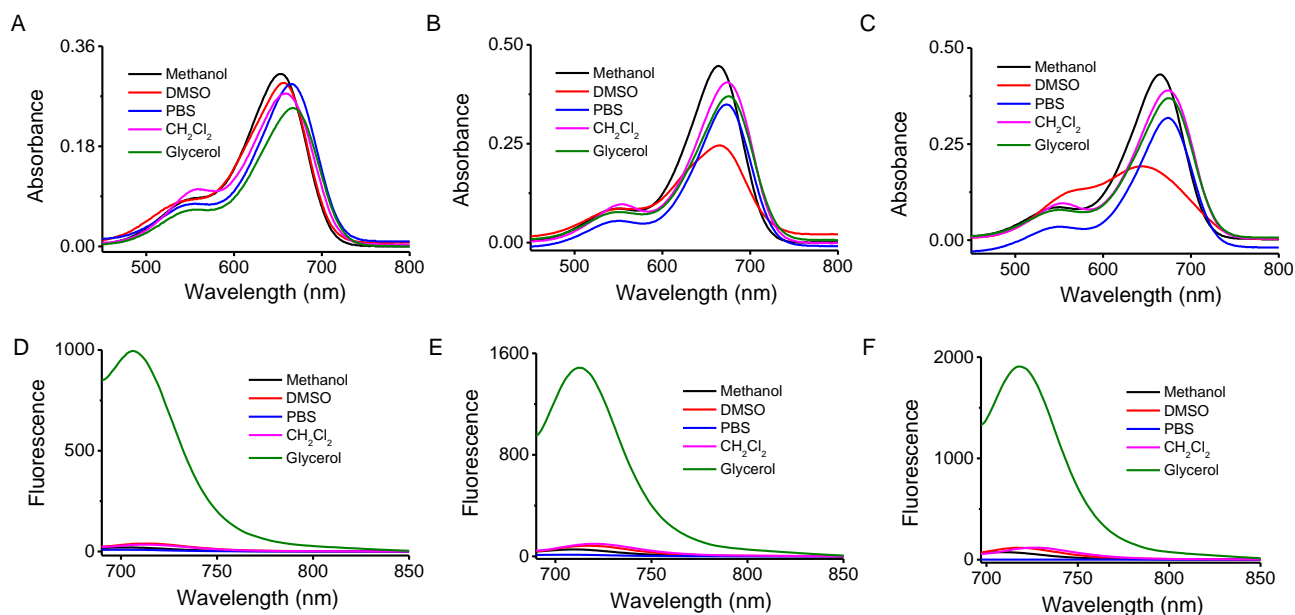


**Fig. S7** The absorption spectra of 5  $\mu\text{M}$  of MYN-MS (A), MYN-BS (B) or MYN-OS (C) in different solvents. The fluorescence spectra of 5  $\mu\text{M}$  of MYN-MS (D), MYN-BS (E) or MYN-OS (F) in different solvents.  $\lambda_{\text{ex/em}} = 670/710$  nm.

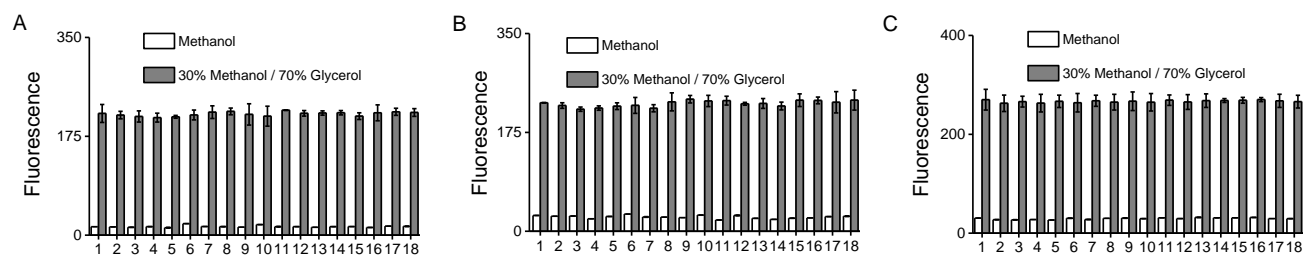


**Fig. S8.** Effects of various reactive oxygen species and biologically relevant species on the fluorescence of 1  $\mu\text{M}$  of MYN-MS (A), MYN-BS (B) and MYN-OS (C) in methanol or the mixed solvent system of methanol/glycerol (3:7, v/v). (1) Probe only; (2) 100  $\mu\text{M}$   $\text{H}_2\text{O}_2$ ; (3)  $\bullet\text{OH}$ : 10  $\mu\text{M}$   $\text{FeSO}_4 + 100$   $\mu\text{M}$   $\text{H}_2\text{O}_2$ ; (4) 1  $\mu\text{M}$   $\text{O}_2^{\bullet-}$ ; (5) 10  $\mu\text{M}$   $\text{HOCl}$ ; (6) 150 mM  $\text{KCl}$ ; (7) 100  $\mu\text{M}$   $\text{CuCl}_2$ ; (8) 2 mM  $\text{CaCl}_2$ ; (9) 2.5 mM  $\text{MgCl}_2$ ; (10) 100  $\mu\text{M}$   $\text{ZnCl}_2$ ; (11) 100  $\mu\text{M}$   $\text{FeCl}_3$ ; (12) 100  $\mu\text{M}$   $\text{FeCl}_2$ ; (13) 1 mM vitamin C; (14) 1 mM GSH; (15) 1 mM cysteine; (16) 1 mM glycine; (17) 10 mM glucose; (18) 100  $\mu\text{g/mL}$  bovine serum albumin.  $\lambda_{\text{ex/em}} = 670/710$  nm.

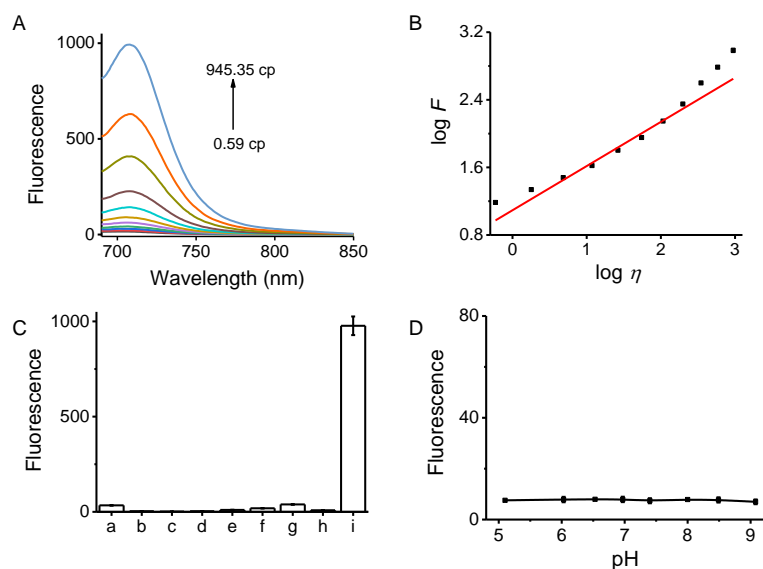


**Fig. S9** (A) Fluorescence emission spectra of MYN-MS (5  $\mu\text{M}$ ) in methanol-glycerol mixtures with different viscosity (from bottom to top, v/v): methanol only; 9:1, 8:2; 7:3; 6:4; 5:5; 4:6; 3:7; 2:8; 1:9; glycerol only. (B) The linear relationship between fluorescence intensity ( $F$ ) and viscosity ( $\eta$ ), which is described with Förster-Hoffmann equation ( $\log F = 0.50 \log \eta + 1.06$ ,  $R^2 = 0.960$ ). (C) Fluorescence intensity of 5  $\mu\text{M}$  MYN-MS in various solvents (a-i):  $\text{CH}_2\text{Cl}_2$ , tetrahydrofuran, ethyl acetate, 1,4-dioxane,  $\text{CH}_3\text{CN}$ , methanol, DMSO, PBS, and glycerol. (D) Effects of pH change of PBS from 5 to 9 on the fluorescence of 5  $\mu\text{M}$  MYN-MS.  $\lambda_{\text{ex/em}} = 670/710$  nm.

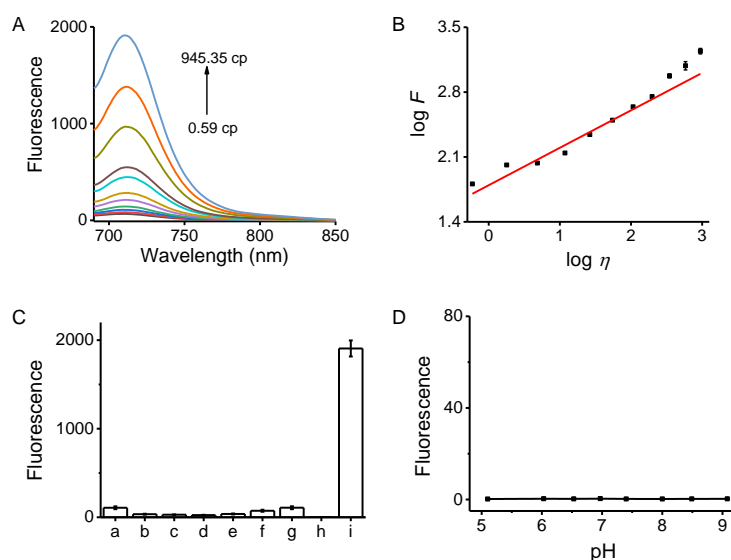


**Fig. S10** (A) Fluorescence emission spectra of MYN-OS (5  $\mu\text{M}$ ) in methanol-glycerol mixtures with different viscosity (from bottom to top, v/v): methanol only; 9:1, 8:2; 7:3; 6:4; 5:5; 4:6; 3:7; 2:8; 1:9; glycerol only. (B) The linear relationship between fluorescence intensity ( $F$ ) and viscosity ( $\eta$ ), which

is described with Förster-Hoffmann equation ( $\log F = 0.40 \log \eta + 1.79$ ,  $R^2 = 0.957$ ). (C) Fluorescence intensity of 5  $\mu\text{M}$  MYN-OS in various solvents (a-i):  $\text{CH}_2\text{Cl}_2$ , tetrahydrofuran, ethyl acetate, 1,4-dioxane,  $\text{CH}_3\text{CN}$ , methanol, DMSO, PBS, and glycerol. (D) Effects of pH change of PBS from 5 to 9 on the fluorescence of 5  $\mu\text{M}$  MYN-OS.  $\lambda_{\text{ex/em}} = 670/710$  nm.

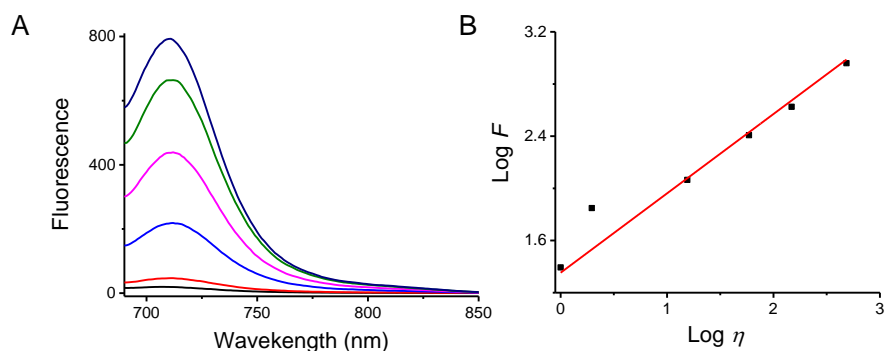


**Fig. S11** (A) Fluorescence spectra of MYN-BS (5  $\mu\text{M}$ ) in sucrose solutions with different viscosities (as described in Table S3). (B) Linear relationship between fluorescence intensity ( $F$ ) and viscosity ( $\eta$ ), which is described with Förster-Hoffmann method ( $\log F = 0.56 \log \eta + 1.41$ ,  $R^2 = 0.990$ ).  $\lambda_{\text{ex/em}} = 670/710$  nm.

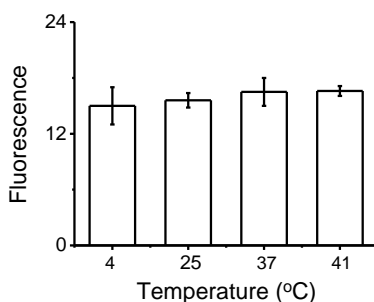


**Fig. S12** Effects of temperature on the fluorescence intensity of 5  $\mu\text{M}$  MYN-BS in pH 7.4 PBS.  $\lambda_{\text{ex/em}} = 670/710$  nm.

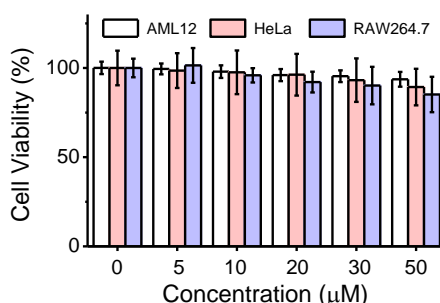


**Fig. S13** Viability of AML12, HeLa and RAW264.7 cells treated with different concentrations of MYN-BS at 37  $^{\circ}\text{C}$  for 24 h. The cell viability without MYN-BS is defined as 100%. The results are given as mean  $\pm$  standard deviation ( $n = 5$ ).

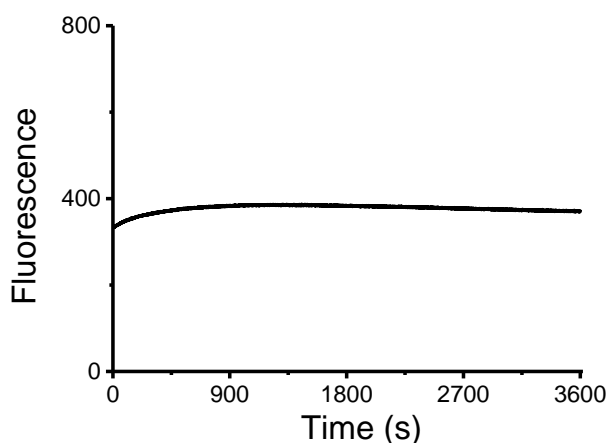


**Fig. S14** Photostability of 5  $\mu\text{M}$  MYN-BS in the mixture of methanol/glycerol (4:6; v/v) at room temperature under continuous 670-nm light illumination.  $\lambda_{\text{em}} = 710$  nm.

**Table S1.** Photophysical data of MYN-MS, MYN-BS and MYN-OS at 25 °C.

Dye	Solvent	$\lambda_{\text{abs}}$ (nm) <sup>[a]</sup>	$\epsilon$ ( $10^4 \text{ M}^{-1}\text{cm}^{-1}$ ) <sup>[b]</sup>	$\lambda_{\text{em}}$ (nm) <sup>[c]</sup>	$\Phi$ (%) <sup>[d]</sup>
MYN-MS	CH <sub>2</sub> Cl <sub>2</sub>	658	5.58	711	1.96
	PBS	664	5.84	704	0.19
	Methanol	651	6.20	705	0.40
	DMSO	655	5.88	712	0.82
	Glycerol	666	4.98	706	27.0
MYN-BS	CH <sub>2</sub> Cl <sub>2</sub>	673	8.10	721	2.99
	PBS	672	6.98	704	0.18
	Methanol	664	8.94	708	1.79
	DMSO	665	4.92	716	1.92
	Glycerol	675	7.40	712	39.0
MYN-OS	CH <sub>2</sub> Cl <sub>2</sub>	674	8.60	718	2.72
	PBS	673	6.96	710 (nearly flat)	0.09
	Methanol	664	8.72	709	1.40
	DMSO	656	3.54	716	1.06
	Glycerol	673	7.52	711	31.5

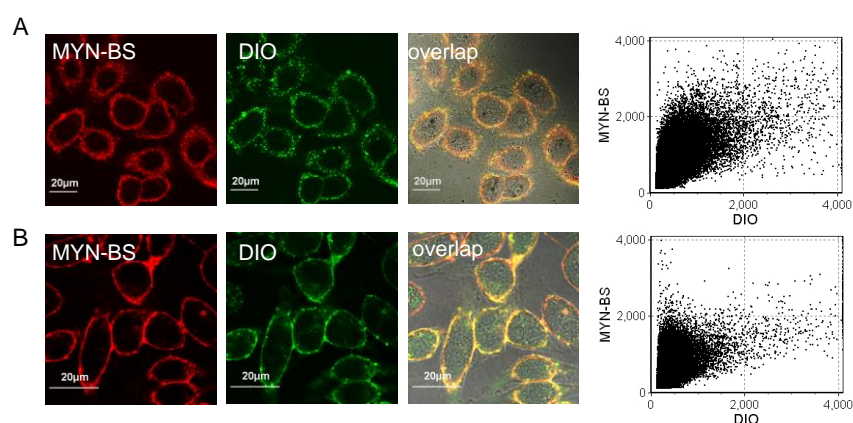
<sup>[a]</sup>Absorption peak. <sup>[b]</sup>Molar absorptivity of the corresponding absorption peak. <sup>[c]</sup>Fluorescence emission peak. <sup>[d]</sup>Fluorescence quantum yield.<sup>5</sup> Cy5 [ $\Phi = 0.27$  in PBS] was used as a standard.

**Table S2.** The viscosity of the methanol-glycerol mixture in different proportions.<sup>6</sup>

methanol (v%)	glycerol (v%)	viscosity (cP)	methanol (v%)	glycerol (v%)	viscosity (cP)
100	0	0.59	40	60	107
90	10	1.79	30	70	198
80	20	4.83	20	80	348
70	30	11.8	10	90	584
60	40	26.4	1	99	945
50	50	55			

**Table S3.** The viscosity of sucrose solutions at different concentrations at 20 °C.<sup>7</sup>

Sucrose concentration (g/100 g water)	Viscosity (cP)
0	1
20	1.96
50	15.5
60	58.9
65	148
70	485

**Fig. S15** Colocalization images of HeLa cells (A) and RAW264.7 cells (B) stained with 10  $\mu$ M of MYN-BS and DIO, and the correlation of MYN-BS and DIO intensities. Scale bars: 20  $\mu$ m. The overlap coefficients are 0.87 and 0.84 for HeLa and RAW264.7 cells, respectively. Red channel:  $\lambda_{\text{ex}} = 635$  nm,  $\lambda_{\text{em}} = 650$ -750 nm; green channel:  $\lambda_{\text{ex}} = 488$  nm,  $\lambda_{\text{em}} = 500$ -550 nm.

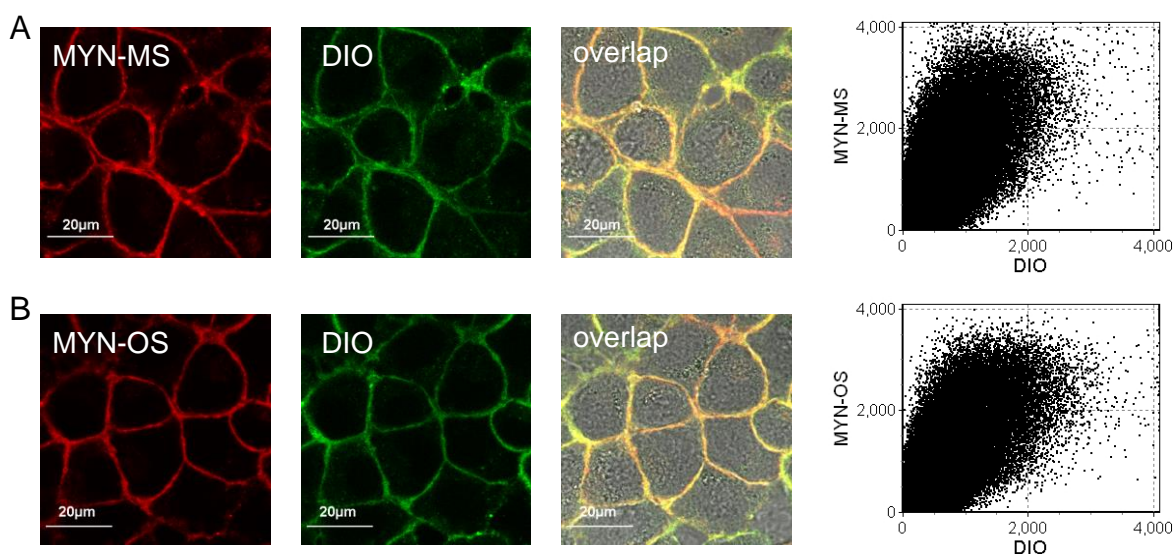


**Fig. S16** Colocalization images of AML12 cells. (A) Cells stained with 10  $\mu\text{M}$  of MYN-MS and DIO, and the correlation of MYN-MS and DIO intensities (overlap coefficient 0.86). (B) Cells stained with 10  $\mu\text{M}$  of MYN-OS and DIO, and the correlation of MYN-OS and DIO intensities (overlap coefficient 0.86). Red channel:  $\lambda_{\text{ex}} = 635 \text{ nm}$ ,  $\lambda_{\text{em}} = 650\text{-}750 \text{ nm}$ ; green channel:  $\lambda_{\text{ex}} = 488 \text{ nm}$ ,  $\lambda_{\text{em}} = 500\text{-}550 \text{ nm}$ . Scale bars: 20  $\mu\text{m}$ .

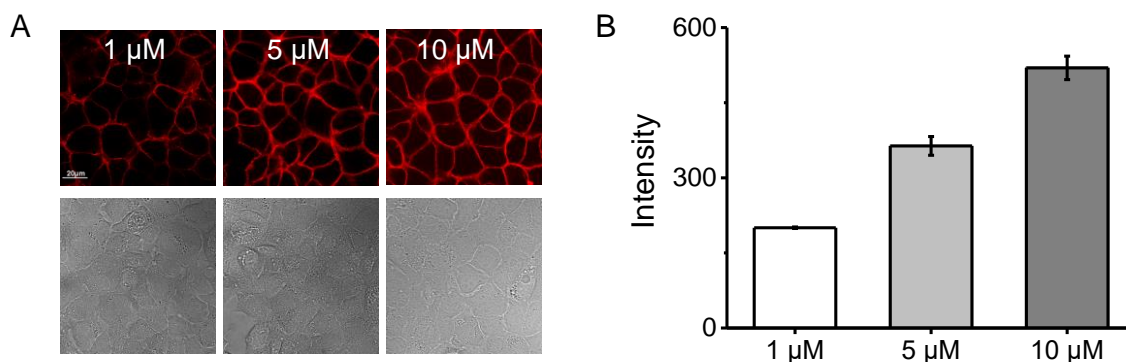


**Fig. S17** Fluorescence images of AML12 cells with MYN-BS at different concentrations of 1, 5 and 10  $\mu\text{M}$ , respectively. The differential interference contrast (DIC) images are shown in the second row. (B) The pixel intensity of the fluorescence images in panel A. Scale bar: 20  $\mu\text{m}$ .  $\lambda_{\text{ex}} = 635 \text{ nm}$ ,  $\lambda_{\text{em}} = 650\text{-}750 \text{ nm}$ .

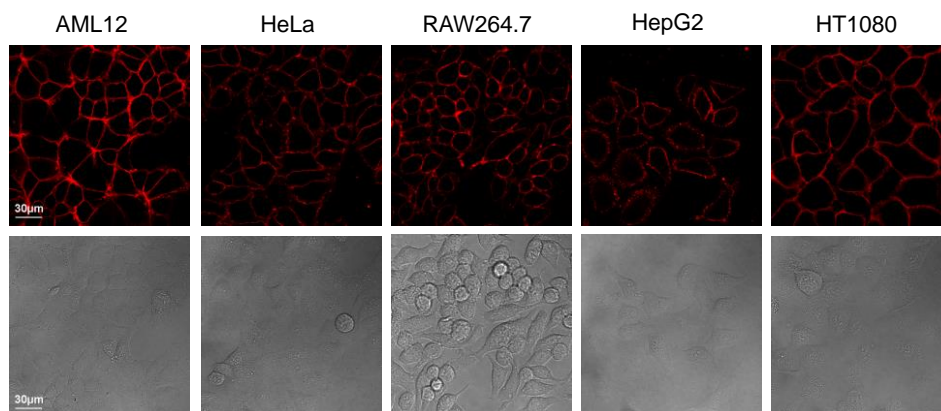


**Fig. S18** Fluorescence and DIC images of AML12, HeLa, RAW264.7, HepG2, and HT1080 cells stained with 10  $\mu\text{M}$  MYN-BS. Scale bars: 30  $\mu\text{m}$ .  $\lambda_{\text{ex}} = 635 \text{ nm}$ ,  $\lambda_{\text{em}} = 650\text{-}750 \text{ nm}$ .

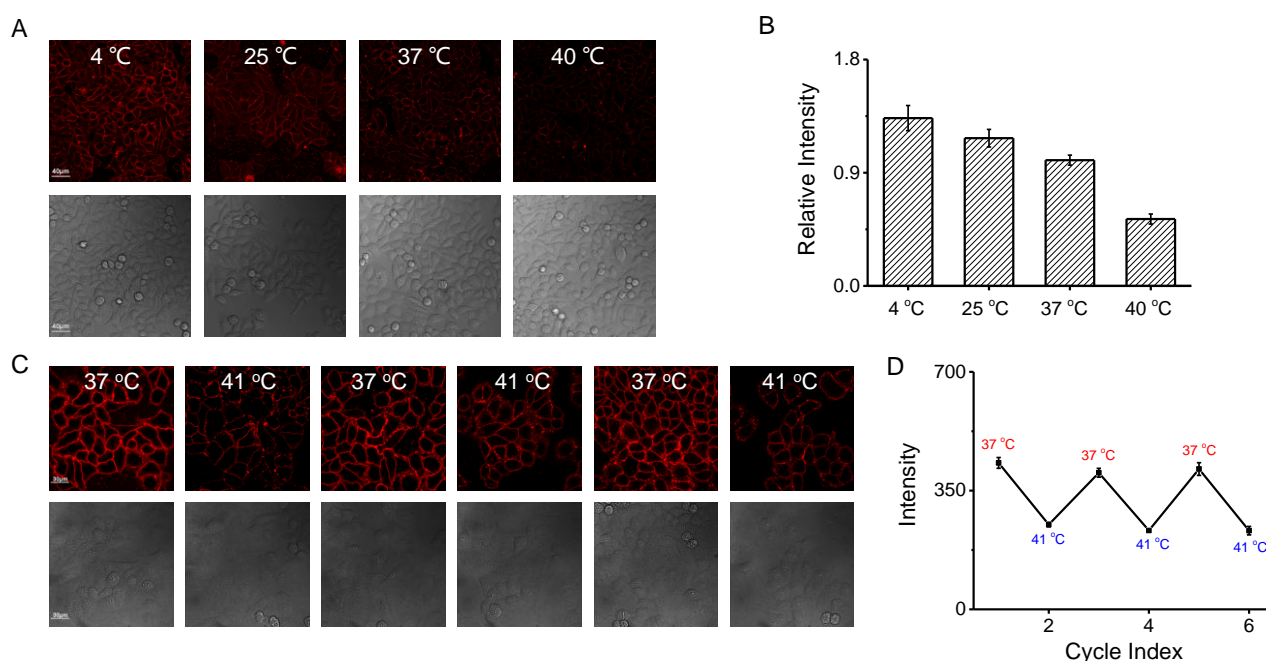


**Fig. S19** Fluorescence imaging of cell membrane viscosity at different temperatures in HeLa cells with 10  $\mu\text{M}$  MYN-BS. The corresponding DIC images are shown in the second row.  $\lambda_{\text{ex}} = 635 \text{ nm}$ ,  $\lambda_{\text{em}} = 650\text{-}750 \text{ nm}$ . (A) Cells incubated with MYN-BS for 20 min at 4 °C, 25 °C, 37 °C and 40 °C. Scale bars: 40  $\mu\text{m}$ . (B) Relative pixel intensity of the corresponding fluorescence images in panel A. The intensity from the image at 37 °C is defined as 1.0. (C) Reversible fluorescence images of cell-membrane viscosity between 37 °C and 41 °C. Scale bars: 30  $\mu\text{m}$ . (D) The pixel intensity of fluorescence images in panel C.

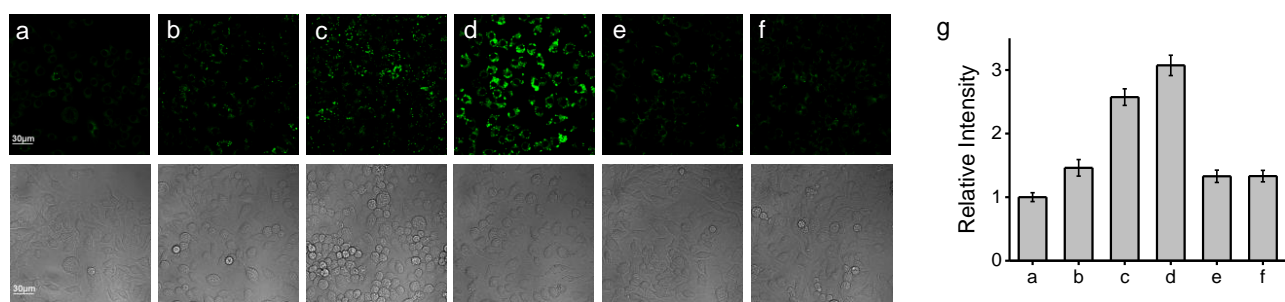


**Fig. S20** Nile red staining experiments of RAW264.7 and macrophage-derived foam cells. (a-d) Cells incubated with (a) 0, (b) 20, (c) 50 or (d) 100  $\mu\text{g/mL}$  of ox-LDL for 24 h, and then with 1  $\mu\text{M}$  Nile red for 15 min. The images e and f represent the cells pretreated with 100  $\mu\text{g/mL}$  ox-LDL for 24 h in the presence of TMN355 (2  $\mu\text{M}$ ) and ezetimibe (10  $\mu\text{g/mL}$ ), respectively, and then with Nile red. (g) The relative pixel intensity of the corresponding fluorescence images a-f (the pixel intensity from image a is defined as 1.0). The DIC images are shown in the second row. The results are presented as mean  $\pm$  standard deviation ( $n = 5$ ). Scale bars: 30  $\mu\text{m}$ .  $\lambda_{\text{ex}} = 488 \text{ nm}$ ,  $\lambda_{\text{em}} = 500\text{-}600 \text{ nm}$ .

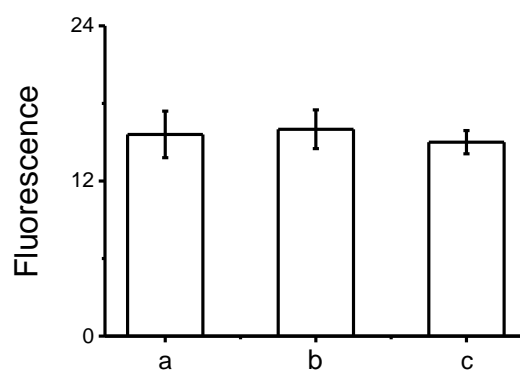


**Fig. S21** Effects of inhibitors (TMN355 and ezetimibe) on the fluorescence intensity of 10  $\mu\text{M}$  MYN-BS in pH 7.4 PBS. (a) Control (probe only); (b) 2  $\mu\text{M}$  TMN355; (c) 10  $\mu\text{g/mL}$  ezetimibe.  $\lambda_{\text{ex/em}} = 670/710 \text{ nm}$ .

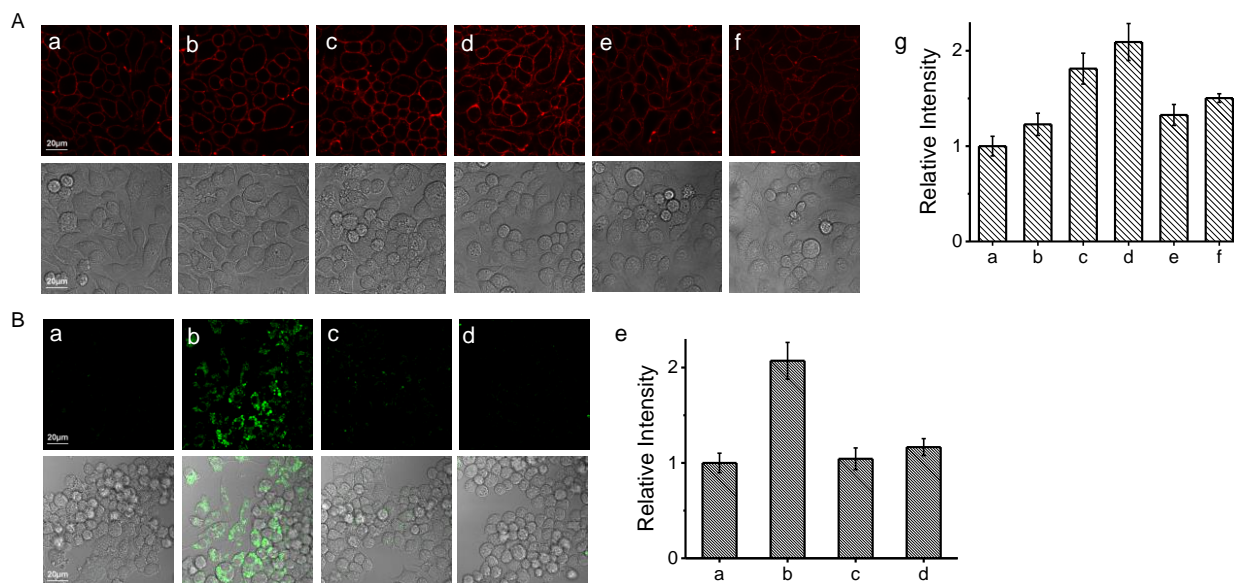


**Fig. S22** (A) Macrophage-derived foam cells incubated with 50 mg/L ox-LDL for 0 (a), 12 (b), 18 (c), or 24 h (d), and then with 10  $\mu$ M MYN-BS. The images e and f represent the cells treated as above for 24 h in the presence of 2  $\mu$ M TMN355 and 10  $\mu$ g/mL ezetimibe, respectively. (g) The relative pixel intensity of the corresponding fluorescence images a-f (the pixel intensity from image a is defined as 1.0).  $\lambda_{\text{ex}} = 635$  nm,  $\lambda_{\text{em}} = 650-750$  nm. (B) Nile red staining experiments of RAW264.7 and macrophage-derived foam cells: (a) RAW264.7 cells incubated with 1  $\mu$ M Nile red; (b) cells pre-incubated with 50 mg/L ox-LDL for 24 h and then with Nile red. The images c and d represent the cells treated 50 mg/L ox-LDL for 24 h in the presence of 2  $\mu$ M TMN355 and 10  $\mu$ g/mL ezetimibe, respectively. (e) The relative pixel intensity of the corresponding fluorescence images a-d (the pixel intensity from image a is defined as 1.0). The corresponding DIC images are shown in the second row. The results are presented as mean  $\pm$  standard deviation ( $n = 5$ ). Scale bars: 20  $\mu$ m.  $\lambda_{\text{ex}} = 488$  nm,  $\lambda_{\text{em}} = 500-600$  nm.

## 8. References

1. L. F. Lu, B. H. Li, S. W. Ding, Y. Fan, S. F. Wang, C. X. Sun, M. Y. Zhao, C. X. Zhao, F. Zhang, *Nat. Commun.*, 2020, **11**, 4192-4202.
2. M. Zheng, D. T. Zhang, M. X. Sun, Y. P. Li, T. L. Liu, S. F. Xue and W. J. Yang, *J. Mater. Chem. C*, 2014, **2**, 1913-1920.

3. Q. Q. Wan, S. M. Chen, W. Shi, L. H. Li and H. M. Ma, *Angew. Chem. Int. Ed.*, 2014, **53**, 10916-10920.
4. P. Greenspan, E. P. Mayer, S. D. Fowler, *J. Cell Biol.*, 1985 **100**, 965-973.
5. R. B. Mujumdar, L. A. Ernst, S. R. Mujumdar, C. J. Lewis, A. S. Waggoner, *Bioconj. Chem.*, 1993, **4**, 105-111.
6. (a) H. Y. Li, W. Shi, X. H. Li, Y. M. Hu, Y. Fang, H. M. Ma, *J. Am. Chem. Soc.* 2019, **141**, 18301-18307; (b) Z. G. Yang, Y. X. He, J. H. Lee, N. Park, M. Suh, W. S. Chae, J. F. Cao, X. J. Peng, H. Jung, C. Kang, J. S. Kim, *J. Am. Chem. Soc.* 2013, **135**, 9181-9185.
7. P. Honig, *Principles of Sugar Technology*; Elsevier Pub. Co., 1953. ISBN: 978-1-4832-3252-2.